Paclitaxel-induced peripheral neuropathy is caused by epidermal ROS and mitochondrial damage through conserved MMP-13 activation

Anthony M. Cirrincione[1#], Adriana D. Pellegrini[2#], Jessica R. Dominy[2], Marisa E. Benjamin[1], Irina Utkina-Sosunova[3], Francesco Lotti[3], Stanislava Jergova[4], Jacqueline Sagen[4], and Sandra Rieger[1*]

[1] University of Miami, Department of Biology, Sylvester Comprehensive Cancer Center at the Miller School of Medicine, 1301 Memorial Drive, Coral Gables, FL 33146

[2] MDI Biological Laboratory, 159 Old Bar Harbor Road, Salisbury Cove, ME 04672

[3] Columbia University Medical Center, Center for Motor Neuron Biology and Disease, Department of Pathology & Cell Biology, 630 West 168th Street, New York, NY 10032

[4] University of Miami, The Miami Project to Cure Paralysis, University of Miami Miller School of Medicine, 1095 Northwest 14th Terrace, Miami

# These authors contributed equally to the manuscript.

*Correspondence to: Sandra Rieger, University of Miami, Department of Biology, 1301 Memorial Drive, Coral Gables, FL 33146, Phone: (305) 284-9935, Fax: (305) 284-3035, E-mail: srieger@miami.edu

Classification: Biological Sciences, Medical Sciences

Keywords
Chemotherapy, neuropathy, paclitaxel, Taxol, MMP, mitochondria, keratinocytes, mammalian

Author Contributions
A.M.C. generated and analyzed data and edited the manuscript.
A.D.P. generated data, analyzed data, and edited the manuscript.
M.B. assisted with cloning and edited the manuscript.
J.D. generated and analyzed data.
S.R. designed the study, generated some of the data, assisted with experimental issues, analyzed the data, and wrote and edited the manuscript.
I.V.U and F.L. generated and analyzed data and edited the manuscript.
S.J. and J.S. generated and analyzed data and edited the manuscript

This PDF file includes:
Main Text
Figures 1 to 4

Abstract

Paclitaxel is a chemotherapeutic agent that causes peripheral neuropathy (PIPN) as a side effect of cancer treatment. Severely affected patients need to terminate chemotherapy, diminishing their chance of survival. The underlying causes of PIPN are unclear, but epidermal, unmyelinated axons have been

shown to be the first to degenerate. We previously utilized a zebrafish *in vivo* model to show that the epidermal matrix-metalloproteinase 13 (MMP-13) induces degeneration of unmyelinated axons, whereas pharmacological inhibition of MMP-13 prevented axon degeneration. The precise functions by which MMP-13 is regulated and affects axons, however, remained elusive. In this study, we assessed mitochondrial damage and reactive oxygen species (ROS) formation as possible inducers of MMP-13, and we analyzed MMP-13-dependent damage. We show that the small ROS, H_2O_2, is increased in keratinocytes following treatment with paclitaxel. Epidermal mitochondrial damage appears to be a source of ROS leading to cytoplasmic H_2O_2 elevation, upregulation of MMP-13, and increased matrix degradation. Intriguingly, although axonal mitochondria also show aberrant morphologies and are vacuolized, as shown in other neuropathies, these axonal mitochondria do not produce increased H_2O_2 levels. We suggest that mitochondrial vacuolization occurs independently of axonal damage given that MMP-13 inhibition prevents axon degeneration, though vacuoles persist. We further show that MMP-13 dysregulation also underlies PIPN in rodent paclitaxel models, and that this function appears to be DRG neuron-extrinsic. These findings suggest that vacuolization is not a cause of paclitaxel-induced neuropathy, and that epidermal MMP-13 is a strong candidate for therapeutic interventions in cancer patients with neuropathy.

Significance statement: Paclitaxel is a chemotherapeutic agent that causes nerve degeneration leading mostly to sensory deficits in the extremities. Severe symptoms such as pain or numbness require patients to terminate chemotherapy, reducing their life expectancy. The mechanisms leading to axon degeneration have been unclear. We show in zebrafish that mitochondrial damage and the release of H_2O_2 in the epidermis, but not in axons, contributes to activation of the matrix-metalloproteinase, MMP-13, in epidermal keratinocytes, leading to matrix degradation and axon degeneration. Pharmacological inhibition of MMP-13 in rodents either by intraperitoneal injection or topical application to the paw pad prevents nerve degeneration and behavioral symptoms. Thus, the epidermis is a major contributor to axon degeneration in both zebrafish and rodents, and likely in humans.

Introduction

Approximately 60-70% of cancer patients treated with paclitaxel develop peripheral neuropathy (1). This condition affects predominantly somatosensory axons in the palms and soles of hands and feet, leading to pain, tingling, temperature sensitivity, and numbness (2, 3). Unmyelinated terminal arbors of somatosensory axons innervating the epidermis have been suggested to be the first to degenerate (4), though the mechanisms leading to their degeneration has remained elusive. We previously showed the conservation of this process in zebrafish, and we mechanistically demonstrated that axon degeneration is mediated by overactivation of the matrix-metalloproteinase, MMP-13 (5). However, the precise mechanism of MMP-13 regulation and the role of MMP-13 in the induction of axon degeneration remained unclear. Scanning electron microscopy indicated that paclitaxel treatment promotes epidermal cell abrasions and adhesion defects, suggesting that increased matrix degradation in the epidermis by MMP-13 may be a cause of axon degeneration whereby axons detach from the matrix due to continuous degradation processes and mechanical stress on the epidermis.

MMP-13 is a member of the matrix-metalloproteinase family of matrix-degrading enzymes. This family has been shown to be regulated by reactive oxygen species (ROS), such as hydrogen peroxide (H_2O_2). For instance, treatment of prostate cancer cells with H_2O_2 elevated *mmp3* expression levels through inhibiting the MMP-3 suppressor, Thrombospondin 2, in a microRNA-dependent manner (6). MMPs can be particularly regulated by mitochondrial ROS (mtROS). For instance, MCF-7 breast cancer cells treated with the mtROS inducer, rotenone, showed increased ROS production and *mmp2* expression. This effect was dependent upon manganese superoxide dismutase (7). The mitochondrial ROS-dependent regulation of MMPs is especially interesting given that paclitaxel treatment directly targets mitochondria, such as in cancer cells (8), and also upregulates MMP-13 in basal keratinocytes in our zebrafish model (5). Since paclitaxel shows strong efficacy in the treatment of carcinomas, an epithelial-derived cancer cell type, this chemotherapeutic agent could similarly induce mitochondrial dysfunction in basal epidermal keratinocytes, leading to MMP-13 upregulation and axon degeneration. Here we assess this idea and analyze how MMP-13 contributes to the degeneration of unmyelinated sensory axons innervating the epidermis.

Results

A prevalent model for paclitaxel neurotoxicity posits that paclitaxel causes axon degeneration by intra-axonal mitochondrial damage and ROS formation (9-11), which parallels findings in cancer cells where paclitaxel treatment *in vitro* induces mitochondrial damage and ROS, ultimately inducing cancer cell apoptosis (8). However, it remains unclear whether the observed mitochondrial damage in axons is a cause of axon degeneration or the consequence of degradation processes induced during axon degeneration (**Figure 1A**). *In vivo* analyses will be useful to dissect this question in more detail using fluorescent genetic H_2O_2 sensors and mitochondrial markers.

We first wanted to analyze whether paclitaxel causes H_2O_2 formation in epidermal keratinocytes and whether H_2O_2 regulates MMP-13 expression. For this, we specifically expressed the H_2O_2 sensor, HyPer (12), in keratinocytes under the *krt4* and *tp63* promoters (5). The *krt4* promoter drives expression in both epidermal layers and is later restricted to differentiated keratinocytes of the surface periderm layer. The *tp63* promoter is restricted to basal epidermal keratinocytes with expression starting around 24hpf when the basal layer forms. HyPer oxidation was measured and represented as the ratio of oxidized to non-oxidized HyPer (**Figure 1B-D**). HyPer oxidation was significantly increased in *tp63* basal keratinocytes of zebrafish treated with paclitaxel over short (3hr) and long-term (2-day) periods (**Figure 1B, C, S1)**. A similar elevation was observed when HyPer was expressed for 5hr and 48hrs under the *krt4* promoter (**Figure 1D, E**). This suggests that paclitaxel elevates H_2O_2 levels in both keratinocyte layers.

Previous studies suggested that wounding such as by fin amputation induces H_2O_2 production in the epidermis (13), and we showed that this process promotes axon regeneration (14). We, therefore, wondered why oxidation in this context is not toxic but pro-regenerative. By comparing amputation induced H_2O_2 levels to those induced by paclitaxel, we noticed that paclitaxel treatment led to continuous H_2O_2 production at steady state in comparison to a transient rise of H_2O_2 during the initial ~20min after amputation followed by declining levels thereafter (**Figure 1E**). Thus, it appears that axons and skin cells

can cope with some exposure to H_2O_2, such as during an injury response, likely due to rapid activation of antioxidant complexes after the initial H_2O_2 production. However, long-term exposure has an opposing effect.

We next wanted to know whether H_2O_2 regulates MMP-13 expression in the context of paclitaxel treatment using western blot analyses. For this, we treated zebrafish either with 0.09% DMSO vehicle (matching the percentage of DMSO contained in the paclitaxel), 23μM paclitaxel plus or minus the antioxidant 1.5mg/L N-acetylcysteine (NAC), and the mitochondrial mtROS inducers rotenone (0.1μM) and paraquat (10μM) for two days (**Figure 1F, G**). The drug doses (except DMSO) reflect the maximally tolerated dose. Compared to vehicle-treated fish, paclitaxel induced the expression of MMP-13 (as previously shown (5)) and this upregulation was reduced below control levels in the presence of NAC. Rotenone and paraquat had the opposite effects. However, rotenone treatment without paclitaxel did not appear to induce MMP-13 expression, which might be a dose-dependent effect. It is also possible that because rotenone induces apoptosis, other pathways in the absence of paclitaxel contributed to the inhibition of MMP-13 expression. Paraquat with and without paclitaxel appeared to increase MMP-13 expression at comparable levels to paclitaxel, suggesting that mtROS might be the sole source of ROS contributing to its expression, whereas cytoplasmic NADPH oxidases are not involved.

To determine how MMP-13 activity affects skin morphology and axon degeneration, we performed transmission electron microscopy (TEM) in zebrafish treated for 96hr (until 6 days post fertilization, dpf) with paclitaxel with and without the MMP-13 inhibitor, DB04760. Treatment with paclitaxel for this period results in prominent axon degeneration (5). This showed paclitaxel-induced basement membrane defects, evidenced by a discontinuous, electron-dense barrier (yellow arrowheads) that separates epidermal basal cells from the underlying dermis (15) (**Figure 1H**). Overall, the tissue appeared less electron-dense, and the keratinocytes in paclitaxel-treated zebrafish appeared loosely attached, as opposed to their tight connections seen in control animals. None of these defects were present when paclitaxel and DB04760 were co-administered. These findings indicate matrix defects as a likely cause of axon degeneration. A pressing question in the field is why axons first begin to degenerate in the hands and feet. Our data suggests the possibility that a combination MMP-13 dependent matrix degradation and increased mechanical stress in the palms and soles might lead to the detachment of axons from the matrix and ultimately causes axonal degeneration.

To determine whether mtROS also cause axon degeneration, consistent with mtROS-dependent MMP-13 upregulation, we quantified intraepidermal branch length following treatment for two days with either vehicle, paclitaxel, paclitaxel+NAC, paclitaxel+rotenone, or paclitaxel+paraquat. We found significant axon degeneration upon paclitaxel treatment with and without rotenone and paraquat, compared with vehicle controls and paclitaxel+NAC treatment, suggesting that paclitaxel induces axon degeneration through mtROS in an MMP-13-dependent manner (**Figure 1I**).

We next wanted to assess whether epidermis-specific mitochondrial damage specifically was the underlying source of mtROS. TEM analysis of mitochondria in basal keratinocytes (**Figure 2A, B**) showed that the cristae and outer and inner membranes appeared less distinct after paclitaxel treatment compared with controls (**Figure S3-5**). We also captured one fusion event of two mitochondria following paclitaxel treatment, which we never observed in the controls (**Figure S4**). Quantification of mitochondria diameter revealed several effects: vehicle-treated mitochondria appeared smaller at 6dpf compared with 2dpa, which could relate to long-term effects of DMSO treatment, or be the result of ongoing developmental changes in the animals, as has been described by others (16). Interestingly, 3hr treatment with paclitaxel led to an acute shrinkage of mitochondria compared with vehicle controls. This effect could not be prevented by co-administration of MMP-13 inhibitors, DB04760, and CL-82198 (**Figure2C**). In contrast, prolonged treatment with paclitaxel led to mitochondrial swelling, whereas co-administration with either of the two MMP-13 inhibitors alleviated the swelling (**Figure 2C**) and restored mitochondrial morphology (**Figure S5**). It is possible that the epidermis remained intact upon MMP-13 inhibition, which also prevented perturbations of mitochondrial function. Thus, mitochondria damage upon long-term exposure to paclitaxel appears to be secondary, while early defects could be a direct effect of paclitaxel.

To further analyze mitochondrial morphology, we tagged keratinocyte-specific mitochondria *in vivo* with mito-dsRed. Measurements of mitochondria length reveled that paclitaxel treatment induced mitochondrial filamentation when analyzed after 3hr, and this effect persisted even after four days of treatment with paclitaxel (**Figure 2D-G**). This data indicates that paclitaxel affects mitochondrial fusion or fission in keratinocytes.

Previous studies investigated mitochondria in DRG axons of rodents treated with paclitaxel, which suggested mitochondrial swelling and vacuolization. These changes were suggested to underlie PIPN (9, 17, 18). To determine if such morphological changes are conserved in zebrafish treated with paclitaxel, we used *in vivo* imaging and TEM analysis (**Figure 3**). Tagging axons with mito-dsRed revealed significant morphological differences, similar to those observed in keratinocytes, namely increased mitochondria diameters suggestive of swelling and enhanced filamentation (**Figure 3A-I**). Intriguingly, despite the increased length of mitochondria, we counted more mitochondria per axon segment in paclitaxel-treated animals compared to controls. These results indicate a possible increase in fusion and fission events to maintain mitochondrial health.

Unlike in keratinocytes, TEM analysis of somatosensory axons within the epidermis showed that mitochondria continue to have distinct outer and inner membranes after treatment with either DMSO vehicle, paclitaxel or paclitaxel+DB04760, or CL-82198 for 3hr and 96hr (**Figure 3J**). Since many axons degenerated after 96hr treatment with paclitaxel, we assume that the remaining axons at this treatment phase are less sensitive to paclitaxel or damage induced in the skin. One possible explanation is that intact axons remain in areas of the skin where the matrix is less degraded. This would be consistent with our finding that only certain patches of basement membrane are degraded while others are still intact. One remarkable finding that our TEM analysis revealed is that, similar to mammalian DRG axons, paclitaxel treatment induced mitochondria vacuolization even after only 3hr treatment. These vacuoles persisted also in mitochondria of axons still present at 96hr of treatment, and in axons of fish in which either MMP-13 inhibitor (DB004760 or CL-82198) was co-administered. Since axon degeneration is prevented in the presence of MMP-13 inhibitors but vacuolization still occurs, it suggests that axonal mitochondrial vacuolization is not an underlying cause of axon degeneration. Moreover, the vacuoles appear rapidly and do not correlate with the onset of axon degeneration that occurs ~3-4 days later, which is substantial given that zebrafish develop from a single embryo into a hatched larva with most organs differentiated by 2dpf. In addition, vacuoles did not appear in keratinocyte mitochondria despite the fact that keratinocytes upregulate MMP-13 and induce axon degeneration. This finding indicates that vacuolization of mitochondria is not a cause of paclitaxel-induced axon degeneration.

Vacuolization has been suggested to induce mitochondrial damage and a disrupted mitochondrial permeability transmission pore in the inner membrane leading to reduced ATP production and mtROS leakage (19). Vacuolization has however also been observed in brown fat and liver tissue of starved rats (20), making it questionable whether these phenotypes are leading to cellular damage. If so, we would expect increased HyPer oxidation in axons. We assessed this by expressing HyPer-cyto under the CREST3 promoter in somatosensory neurons that innervate the epidermis **(Figure 3K)**. To our surprise, we could not detect increased H_2O_2 levels in epidermal sensory axons following paclitaxel treatment for 3hr, 48hr and 96hr. Interestingly, DMSO vehicle did initially, but transiently, increase HyPer oxidation. This effect was however undetectable after prolonged treatment. These data indicate that paclitaxel does not elevate axonal cytoplasmic H_2O_2 levels. The DMSO-dependent elevation of H_2O_2 might be due to increased membrane permeabilization, which could potentially be countered by a paclitaxel-mediated increase in axonal cytoskeletal (microtubule) rigidity.

Because of the similarities to mammalian paclitaxel-induced phenotypes in zebrafish, we wanted to test whether MMP-13-dependent axon degeneration is conserved in mammals. To induce PIPN, we injected rats and mice on alternating days with 2mg/kg and 4mg/kg paclitaxel in Cremophor/NaCl, respectively, over the course of 7 days (cumulative doses of 8mg/kg and 16mg/kg). Some animals received Cremophor/NaCl as vehicle control, or Cremophor/NaCl+CL-82198. As other studies have shown (9, 21-23), we were able to induce mechanical, thermal and cold nociceptive sensitivity in the paclitaxel-injected animals (**Figure 4A-D**). These phenotypes were prevented in paclitaxel-injected animals in which CL-82198 was co-administered. CL-82198/vehicle-injections produced comparable results to those injected

with the vehicle alone. We also analyzed axon degeneration in the dorsal horn of injected rats using CGRP antibody staining, which showed reduced expression upon paclitaxel injections, and this effect was prevented in either vehicle or paclitaxel+CL-82198 injected animals (**Figure S6A-D)**.

We previously showed in zebrafish that MMP-13 expression induced by paclitaxel was restricted to the epidermis and was not found in epidermal axons of sensory neurons (5). To determine whether MMP-13 dependence was neuron-intrinsic in mammals, we cultured mouse DRG neurons and examined neurite degeneration following treatment with DMSO vehicle, paclitaxel, paclitaxel+CL-82198, or paclitaxel+DB04760 at various concentrations. While paclitaxel induced neurite degeneration in the cultures, CL-82198 co-administration did not prevent degeneration, suggesting that similar to our zebrafish observations, MMP-13 is not functioning neuron-intrinsically (**Figure 4E-G**). Consistent with a skin-specific role for MMP-13, we found that topical application of 10μM CL-82198 to the hind paw of rats injected with paclitaxel led to a faster recovery from allodynia and cold sensitivity (**Figure 4H, I**). Thus, these findings indicate that MMP-13-dependent epidermal activity is conserved in both zebrafish and mammals, and likely also contributes to PIPN in human patients.

Discussion

Our data suggests a model by which epidermal mitochondrial damage induces H_2O_2 production leading to increased MMP-13-dependent matrix degradation and axon degeneration (**Figure S7**). Mitochondria in the epidermis, and also in sensory axons, appear to be elongated upon paclitaxel treatment, likely related to defects in the fusion or fission machinery. Previous studies showed that H_2O_2 promotes mitochondrial fission, but our data points to increased filamentation, arguing against a model in which H_2O_2 damages mitochondria. Instead, mitochondrial damage appears to cause H_2O_2/ROS formation leading to downstream effects, such as MMP-13 activation. Strikingly, although mitochondria damage similarly occurs in axons, we don't believe this to be the cause of axon degeneration. We showed that pharmacological MMP-13 inhibition can prevent axon degeneration (5), yet, MMP-13 inhibition does not prevent axonal mitochondrial vacuolization and morphological changes. It is also interesting that axons accumulate elongated mitochondria but at the same time significantly increase the number of mitochondria per branch segment. It is possible that axons have an increased ability to undergo fusion and fission at an accelerated rate as a means to increase mitochondrial health, whereas this ability is inhibited in keratinocytes.

Why do epidermal mitochondria contribute to MMP-13 expression, but sensory neurons do not upregulate MMP-13? The simplest explanation is that regulatory elements leading to MMP-13 expression are not present in these neurons, and thus axons cannot upregulate MMP-13. This is consistent with our mouse DRG *in vitro* culture data (**Figure 4E-G**). However, it has been well established that H_2O_2/ROS can upregulate other MMPs, which could in principle contribute to axon degeneration. But because H_2O_2/ROS levels are low, as determined in our HyPer experiments (**Figure 3K**), MMPs won't be activated in the context of paclitaxel treatment. Another pertinent question is why axons have low H_2O_2/ROS levels while keratinocytes do not. Perhaps axons have the ability to better regulate H_2O_2/ROS through means of antioxidant complexes that scavenge H_2O_2/ROS. Evidence for this theory stems from the fact that axons can survive and even regenerate upon exposure to injury-released H_2O_2/ROS from keratinocytes (14) whereas keratinocytes that are exposed to prolonged H_2O_2/ROS levels might be more vulnerable to damage. Thus, epidermis-innervating somatosensory neurons must have evolved a better mechanism to tolerate long-term exposure to H_2O_2/ROS levels. This difference could hinge on the H_2O_2-dependent expression of MMP-13. Under conditions of paclitaxel treatment, keratinocytes utilize the same mechanisms of MMP-13 upregulation as after skin injury, where MMP-13 is localized to the leading edge of migrating keratinocytes during the re-epithelialization step of the wound (24). Because MMP-13 actions are transient, this process is coordinated with the healing of the wound, after which H_2O_2/ROS and MMP-13 are downregulated. However, if MMP-13 remains high, continuous matrix degradation under homeostatic conditions will damage epidermal cells and ultimately the axons.

How is mitochondrial damage induced by paclitaxel in keratinocytes and axons? Previous studies demonstrated that paclitaxel can directly damage isolated mitochondria of neuroblastoma cells (8) and liver cells (25), and thus it could also exert direct effects on mitochondria in cell types, such as keratinocytes and axons. This also indicates that microtubule damage, as observed in cells treated with

paclitaxel, may not contribute significantly to axon degeneration. While microtubule damage is a desired effect during cancer treatment, neurons do not divide, and keratinocytes in zebrafish do rarely divide during larval stages. However, basal keratinocytes divide frequently in the mammalian and the adult zebrafish epidermis, and paclitaxel treatment may have additional effects in dividing epithelia that could lead to further damage, though this remains to be shown. Nevertheless, our mammalian data and previous adult zebrafish data (5) showing the reversal of behavioral symptoms and axon degeneration induced by paclitaxel in the presence of MMP-13 inhibitor suggests that MMP-13 is a primary inducer of axon degeneration.

Materials and Methods (see Extended Methods for detailed description)

Animals

Zebrafish and rodents were handled according to good animal practices, as approved by the appropriate IACUC committees at each institution.

Plasmids

The following plasmids were used: UAS-mito-dsRed, *krt4:*Gal4VP16 driver to label skin mitochondria, CREST3:Gal4VP16_14xUAS-GFP to label sensory neurons, *krt4:*HyPer-cyto (5), *tp63*:HyPer, CREST3:Gal4VP16_14x-HyPer-cyto.

Drug administrations

Zebrafish: Starting 2dpf, zebrafish were individually incubated with 0.09% DMSO/Ringers, 23μM pre-made paclitaxel/DMSO (Millipore), 10μM each DB04760 (MMP-13 inhibitor, PubChem CID: 5289110) (sc-205756, Santa Cruz Biotechnology) and CL-82198 (Tocris, USA) in DMSO, 0.1μM Rotenone, 10μM paraquat (Sigma-Aldrich), and 1.5mg/L N-acetylcysteine (Sigma-Aldrich). *Rodents:* Injection of vehicle (Cremophor-EL/EtOH 50/50 diluted into 0.9% NaCl), paclitaxel/vehicle (4x2mg/kg in rats and 4x4mg/kg in mice), vehicle+CL-82198 (5mg/kg) or paclitaxel+CL-82198 (1, 5, or 10mg/kg, as indicated in Figure 4, S6, on Days 1, 3, 5, 7). 10μM CL-82198/0.01% DMSO was topically applied to ipsilateral hind paw once a day for seven days during the injection period.

Antibodies and Fluorescent markers

Western blot: Primary antibodies (1:333, rabbit MMP-13, ProteinTech; 1:2000, mouse anti-beta-actin, Abcam). Fluorescent secondary antibodies (anti-mouse IgG 1:5000 IRDye 680RD; anti-rabbit IgG 1:5000 IRDye 800CW). *Immunofluorescence:* mouse CGRP (1:1000, Millipore) and anti-mouse Alexa flour-633 (1:250, ThermoFisher), DAPI (1:1000, Invitrogen), Hoechst 33347 (Sigma-Aldrich).

Adult mouse DRG cultures

DRGs from cervical, thoracic and lumbar anatomical regions were collected from 8-week adult mouse spinal columns. Neuronal cells were purified from ~50 DRGs and plated at ~7 $x10^4$ in 96-well plates coated with 100μg/ml polyornitine and 10μg/ml laminin.

Behavioral studies

Cold response, Hargreaves (thermal response), and von Frey filament testing was conducted on the following days: pre-injection, day 2, 4, 7, 9, 11, 14, 16, and 23. Animals were sacrificed on day 23. The data was analyzed using a Dixon nonparametric test and expressed as the paw withdrawal threshold in gram force values (26). The group means and standard error of the mean (SEM) were calculated and graphed.

Statistical analyses

Statistical comparisons were made using Prism8 (GraphPad) and Student's t-test or one-way ANOVA at an alpha=0.05 (95% confidence interval). Tuckey's multiple comparisons post-tests were used. Significance is denoted with asterisks: *$p<0.05$, **$p<0.01$, ***$p<0.001$, ****$p<0.0001$. The standard error of the mean (S.E.M.) is shown, reflecting comparisons of groups of several animals or procedures in multiple biological replicates.

Acknowledgments
We thank Pete Finger at The Jackson Laboratory for his assistance with the TEM studies. We also thank the fish facility staff at MDI Biological Laboratory and the University of Miami for their excellent zebrafish care. The authors do not declare any conflicts of interest.

Funding sources
Research reported in this publication was sponsored by the following grants from the National Institutes of Health: NINDS R21-NS094939, NCI R01CA215973, and NIGMS P20GM0103423 and P20GM104318 awarded to MDI Biological Laboratory, P20GM103643 awarded to the University of New England and the Behavioral Core, and Miami-CTSI Award. Additional funding was provided by SG5598 Maine Technology Institute. Dr. Rieger is the guarantor of this work and, as such, had full access to all the data in the study and takes responsibility for the integrity of the data and the accuracy of the data analysis.

References

1. M. Seretny *et al.*, Incidence, prevalence, and predictors of chemotherapy-induced peripheral neuropathy: A systematic review and meta-analysis. *Pain* **155**, 2461-2470 (2014).

2. P. A. Forsyth *et al.*, Prospective study of paclitaxel-induced peripheral neuropathy with quantitative sensory testing. *J Neurooncol* **35**, 47-53 (1997).

3. S. B. Park *et al.*, Early, progressive, and sustained dysfunction of sensory axons underlies paclitaxel-induced neuropathy. *Muscle Nerve* **43**, 367-374 (2011).

4. G. J. Bennett, G. K. Liu, W. H. Xiao, H. W. Jin, C. Siau, Terminal arbor degeneration--a novel lesion produced by the antineoplastic agent paclitaxel. *Eur J Neurosci* **33**, 1667-1676 (2011).

5. T. S. Lisse *et al.*, Paclitaxel-induced epithelial damage and ectopic MMP-13 expression promotes neurotoxicity in zebrafish. *Proc Natl Acad Sci U S A* **113**, E2189-2198 (2016).

6. C. L. Hsieh *et al.*, Reactive oxygen species-mediated switching expression of MMP-3 in stromal fibroblasts and cancer cells during prostate cancer progression. *Sci Rep* **7**, 9065 (2017).

7. H. J. Zhang *et al.*, Activation of matrix metalloproteinase-2 by overexpression of manganese superoxide dismutase in human breast cancer MCF-7 cells involves reactive oxygen species. *J Biol Chem* **277**, 20919-20926 (2002).

8. N. André *et al.*, Paclitaxel targets mitochondria upstream of caspase activation in intact human neuroblastoma cells. *FEBS Lett* **532**, 256-260 (2002).

9. S. J. Flatters, G. J. Bennett, Studies of peripheral sensory nerves in paclitaxel-induced painful peripheral neuropathy: evidence for mitochondrial dysfunction. *Pain* **122**, 245-257 (2006).

10. A. Areti, V. G. Yerra, V. Naidu, A. Kumar, Oxidative stress and nerve damage: role in chemotherapy induced peripheral neuropathy. *Redox Biol* **2**, 289-295 (2014).

11. N. A. Duggett *et al.*, Oxidative stress in the development, maintenance and resolution of paclitaxel-induced painful neuropathy. *Neuroscience* **333**, 13-26 (2016).

12. V. V. Belousov *et al.*, Genetically encoded fluorescent indicator for intracellular hydrogen peroxide. *Nat Methods* **3**, 281-286 (2006).

13. P. Niethammer, C. Grabher, A. T. Look, T. J. Mitchison, A tissue-scale gradient of hydrogen peroxide mediates rapid wound detection in zebrafish. *Nature* **459**, 996-999 (2009).

14. S. Rieger, A. Sagasti, Hydrogen peroxide promotes injury-induced peripheral sensory axon regeneration in the zebrafish skin. *PLoS Biol* **9**, e1000621 (2011).

15. D. Le Guellec, G. Morvan-Dubois, J. Y. Sire, Skin development in bony fish with particular emphasis on collagen deposition in the dermis of the zebrafish (Danio rerio). *Int J Dev Biol* **48**, 217-231 (2004).

16. B. S. Weakley, Variations in mitochondrial size and ultrastructure during germ cell development. *Cell Tissue Res* **169**, 531-550 (1976).

17. H. W. Jin, S. J. Flatters, W. H. Xiao, H. L. Mulhern, G. J. Bennett, Prevention of paclitaxel-evoked painful peripheral neuropathy by acetyl-L-carnitine: effects on axonal mitochondria, sensory nerve fiber terminal arbors, and cutaneous Langerhans cells. *Exp Neurol* **210**, 229-237 (2008).

18. H. Zheng, W. H. Xiao, G. J. Bennett, Functional deficits in peripheral nerve mitochondria in rats with paclitaxel- and oxaliplatin-evoked painful peripheral neuropathy. *Exp Neurol* **232**, 154-161 (2011).

19. D. B. Zorov, M. Juhaszova, S. J. Sollott, Mitochondrial reactive oxygen species (ROS) and ROS-induced ROS release. *Physiol Rev* **94**, 909-950 (2014).

20. J. D. LEVER, J. B. CHAPPELL, Mitochondria isolated from rat brown adipose tissue and liver. *J Biophys Biochem Cytol* **4**, 287-290 (1958).

21. C. M. Peters *et al.*, Intravenous paclitaxel administration in the rat induces a peripheral sensory neuropathy characterized by macrophage infiltration and injury to sensory neurons and their supporting cells. *Exp Neurol* **203**, 42-54 (2007).

22. R. C. Polomano, A. J. Mannes, U. S. Clark, G. J. Bennett, A painful peripheral neuropathy in the rat produced by the chemotherapeutic drug, paclitaxel. *Pain* **94**, 293-304 (2001).

23. J. Xu *et al.*, Role of Complement in a Rat Model of Paclitaxel-Induced Peripheral Neuropathy. *Journal of Immunology (Baltimore, Md.: 1950)* **200**, 4094-4101 (2018).

24. N. Hattori *et al.*, MMP-13 plays a role in keratinocyte migration, angiogenesis, and contraction in mouse skin wound healing. *Am J Pathol* **175**, 533-546 (2009).

25. G. Varbiro, B. Veres, F. Gallyas, B. Sumegi, Direct effect of Taxol on free radical formation and mitochondrial permeability transition. *Free Radic Biol Med* **31**, 548-558 (2001).

26. S. R. Chaplan, F. W. Bach, J. W. Pogrel, J. M. Chung, T. L. Yaksh, Quantitative assessment of tactile allodynia in the rat paw. *J Neurosci Methods* **53**, 55-63 (1994).

Figure legends

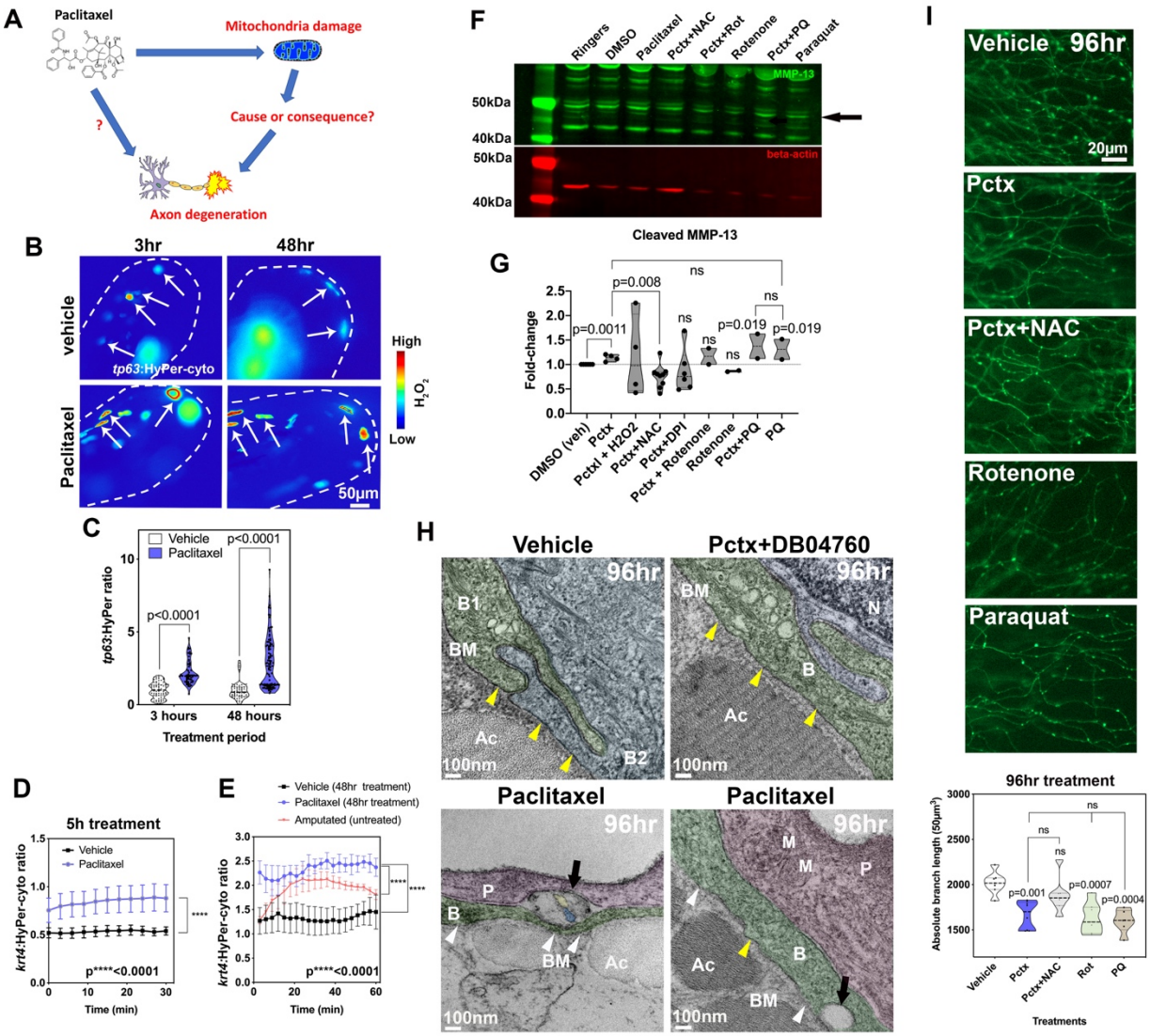

Figure 1. Mitochondrial ROS contribute to MMP-13 expression and axon degeneration. (A) Is mitochondrial damage involved in paclitaxel-induced axon degeneration? **(B)** Ratiometric images showing HyPer oxidation (arrows) in the caudal fin of larval zebrafish (dashed lines) after 3 and 48hr of treatment (2 and 4dpf, respectively) with either 0.09%DMSO vehicle or 23µM paclitaxel. Keratinocytes are mosaically labeled following transient injection of *tp63*:HyPer into 1-cell stage embryos. High oxidation is represented in red and low oxidation in blue. **(C)** Quantification reveals increased oxidation after short and long-term treatment with paclitaxel, n=10 animals. **(D, E)** 30-60 min quantifications of HyPer oxidation in epidermal cells expressing *krt4*:HyPer following treatment for 5 (**D**) and 48hr (**E**), n=3-6 animals, SEM. Paclitaxel treatment significantly elevates H_2O_2 levels. Comparison with H_2O_2 induced by fin amputation shows continuous versus transient H_2O_2 elevation. **(F, G)** Western blot (black arrow indicates cleaved MMP-13, 48kDa) (F) and quantitative analysis (G) shows increased MMP-13 expression following treatment with paclitaxel and the mitochondrial ROS inducer paraquat but not rotenone. Antioxidants (NAC and DPI) reduce MMP-13 levels induced by paclitaxel treatment, n=2 biological replicates with 5-10 animals each treatment. **(H)** TEM of (6dpf) zebrafish keratinocytes following 96hr treatment with either 0.09% DMSO vehicle, 23µM paclitaxel+DB04760 (MMP-13 inhibitor) or paclitaxel alone shows an intact basement membrane (yellow arrowheads) in vehicle and paclitaxel+DB04760 treated fish, whereas the

basement membrane is discontinuous (white arrowheads) and large gaps (black arrows) appear where unmyelinated sensory axons normally reside. **(H)** Epidermal unmyelinated sensory axons in the distal tail fin following 96hr treatment with vehicle, paclitaxel, paclitaxel+NAC, rotenone, or paraquat. Quantification of treatments shows paclitaxel, rotenone, and paraquat induce axon degeneration whereas NAC co-administration prevents degeneration, n=5-7 animals, SEM.
Abbreviations: NAC=N-acetylcysteine, Pctx=paclitaxel, Rot=rotenone, PQ=paraquat, B=basal keratinocyte, BM=basement membrane, Ac=actinotrichia, N=nucleus, P=periderm, M=mitochondrion, dpf=days post fertilization

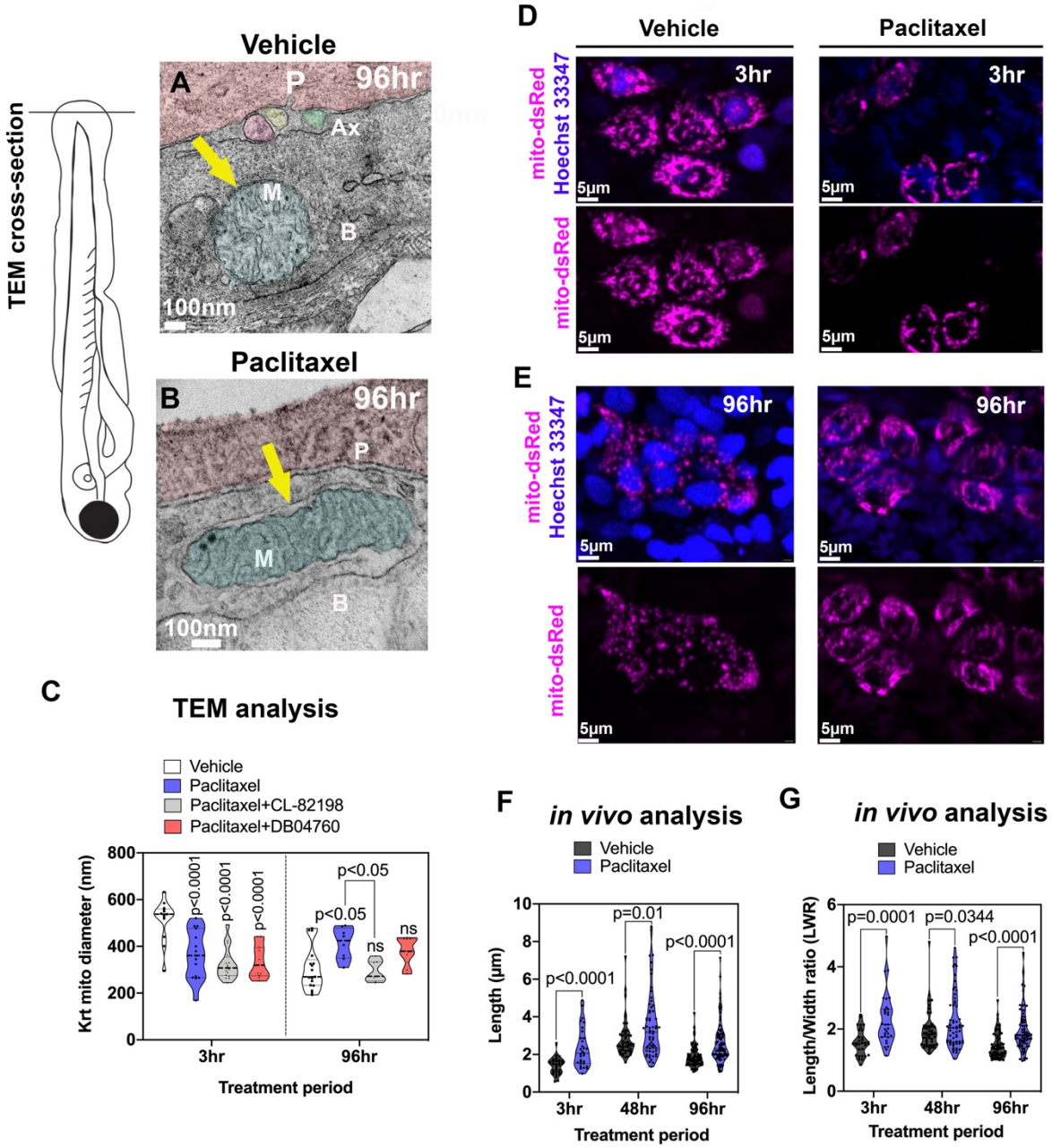

Figure 2. Keratinocyte mitochondria are damaged by paclitaxel treatment. (A) TEM analysis of zebrafish larvae treated for 96hr with either 0.09% DMSO vehicle or 23µM paclitaxel (2-6dpf). A mitochondrion (M) is shown with outer and inner membrane (white arrow) and clearly visible cristae

following vehicle treatment. Three axons (Ax) are embedded between the periderm and basal keratinocyte layer. **(B)** The outer membrane of a mitochondrion following paclitaxel treatment is less apparent, and the space between inner and outer membrane has increased (yellow arrow). The cristae are less electron-dense, and large dark puncta are visible. **(C)** Quantification shows decreased mitochondria diameters upon 3hr paclitaxel treatment with and without MMP-13 inhibitors, CL-82198 or D04760, compared with controls. 96hr treatment shows increased mitochondria diameters in paclitaxel but not MMP-13 inhibitor treated animals, n=3 animals. **(D, E)** *In vivo* imaging of mitochondria in keratinocytes labeled with mito-dsRed and nuclei labeled with live Hoechst 33347 stain following treatment for 3hr and 96hr with either vehicle (**D**) or paclitaxel (**E**). Short and long-term treatment with paclitaxel promotes mitochondria filamentation. **(F, G)** Quantification after 3hr, 48hr and 96hr treatment shows increased length (**F**) and length/width ratios (**G**) with paclitaxel compared to controls, n=5-8 animals. *Abbreviations: B=basal keratinocyte, P=periderm, M=mitochondrion, Ax=axon*

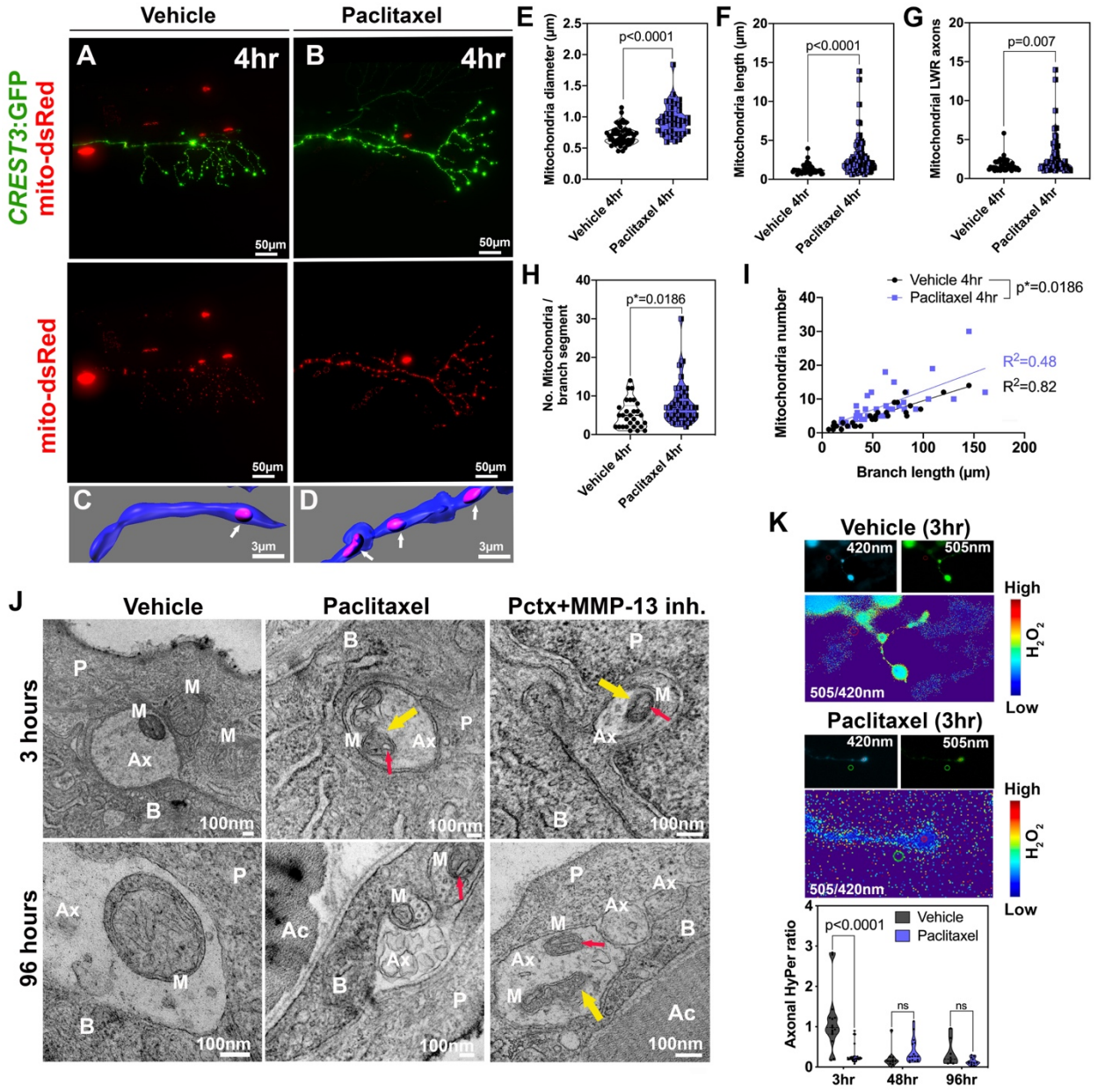

Figure 3. Axonal mitochondria are vacuolized following paclitaxel treatment but ROS/H_2O_2 levels are not elevated. (A, B) DsRed-labeled mitochondria in unmyelinated axons of somatosensory neurons labeled with CREST3:GFP following 4hr treatment with vehicle (**A**) or paclitaxel (**B**). **(C, D)** Respective 3D reconstructions of axon branch segment (blue) in the epidermis containing mitochondria (pink, arrows). **(E-I)** Quantification of axonal mitochondria shows increased diameter (**E**), length (**F**), length-width ratio (**G**) and number of mitochondria per branch segment (**H, I**), n=5 animals. **(J)** TEM analysis of axonal mitochondria (M) following treatment with 0.09% DMSO vehicle, paclitaxel with or without MMP-13 inhibitor (CI-82198 top and DB04760 bottom) for 3hr and 96hr shows rapid paclitaxel-induced mitochondria vacuolization (red arrows) and membrane disruptions (yellow arrows), persisting up to 96hr, similar to paclitaxel+MMP-13 inhibitor. **(K)** Axonal HyPer oxidation is elevated after DMSO treatment for 3hr but not after prolonged treatment with either DMSO or paclitaxel, n=5-7 animals. *Abbreviations: B=basal keratinocyte, P=periderm, M=mitochondrion, Ax=axon, Ac=Actinotrichia*

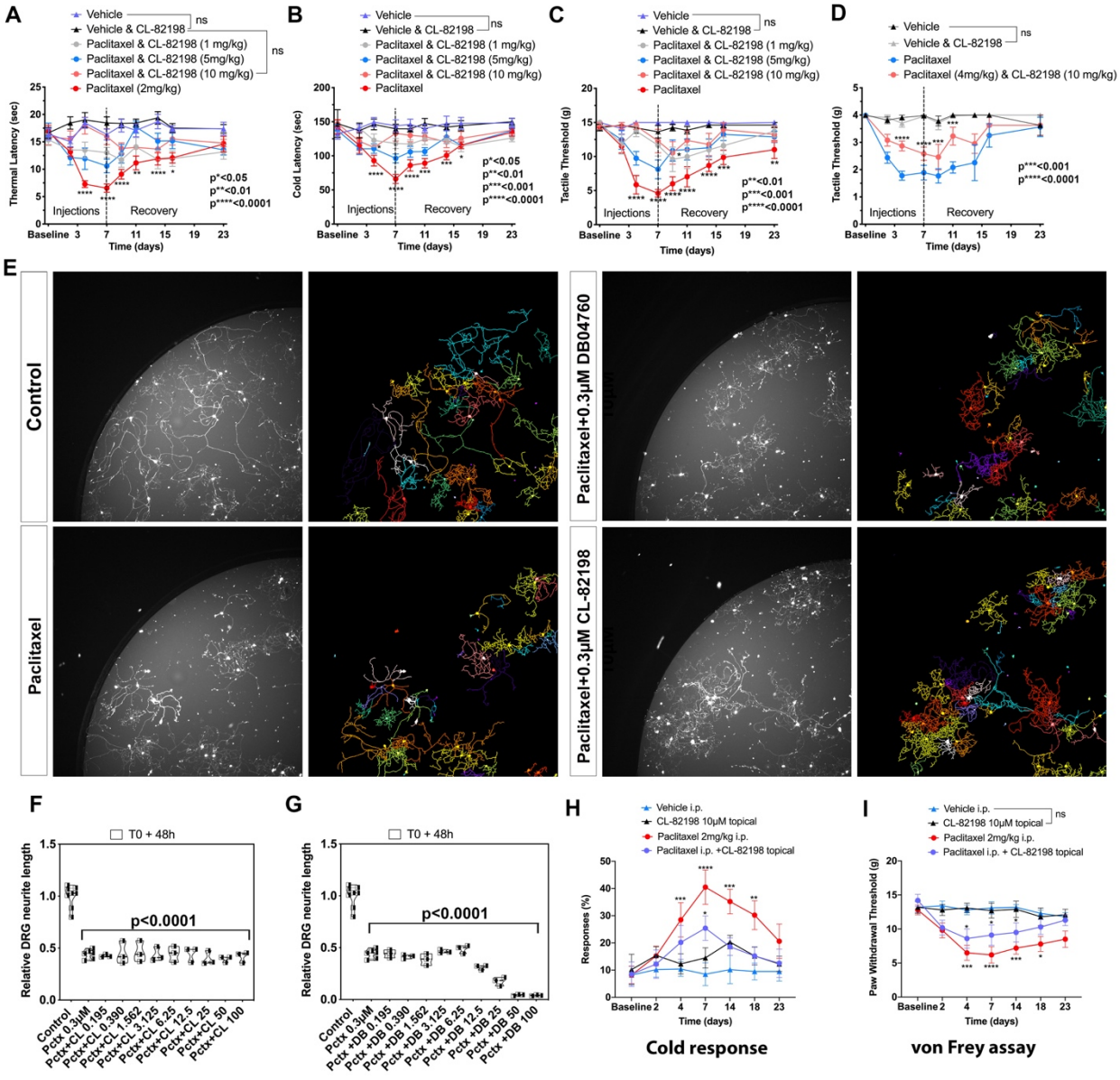

Figure 4. MMP-13 prevents paclitaxel-induced PIPN in rodents by neuron-extrinsic mechanism. (A-D) Increased sensitivity to heat (**A**), cold (**B**) and touch (**C, D**) following paclitaxel treatment of rats (**A-C**) and mice (**D**) compared with controls and upon injection of paclitaxel+CL-82198, n=6-14 animals. **(E-G)** DRG neurite tracings (**E**) and length quantification (**F, G**) shows decreased length upon treatment with either paclitaxel, paclitaxel+CL-82198, or paclitaxel+DB04760, n=3 biological replicates. (**H**, **I**) Increased cold response and tactile sensitivity is alleviated upon topical application of CL-82198 to the hind paw of paclitaxel-injected rats (n=3).